




Cite this: *Phys. Chem. Chem. Phys.*,  
2019, 21, 9883

# Lithium ion diffusion mechanism in covalent organic framework based solid state electrolyte†

Kecheng Zhang, Bingkai Zhang, Mouyi Weng, Jiaxin Zheng, Shunning Li\* and Feng Pan \*

Solid state electrolytes (SSEs) based on two dimensional covalent organic frameworks (2D-COFs) with Li salts and solvents impregnated in their large pores have emerged as novel candidate materials for solid state lithium batteries. Here, using *ab initio* molecular dynamics simulation, we track the atomic-scale structural evolution during Li<sup>+</sup> ion diffusion in a 2D-COF SSE composed of COF-5, LiClO<sub>4</sub> and tetrahydrofuran (THF). Our simulation results show the transient dynamics of the Li<sup>+</sup> diffusion events, the free rotation of ClO<sub>4</sub><sup>-</sup> ions and the essential role of THFs in partitioning between the ions and the solid framework. We find clear evidence that Li<sup>+</sup> ion diffusion adopts a one-dimensional (1D) liquid-like behavior with the coordination evolution driven by facile rotation and short-range diffusion of ClO<sub>4</sub><sup>-</sup> ions and THFs. The fast Li<sup>+</sup> diffusion pathway in the 1D tunnels of COFs may shed light on future design of high-performance COF based SSEs.

Received 15th April 2019,  
Accepted 23rd April 2019

DOI: 10.1039/c9cp02117e

rsc.li/pccp

## Introduction

The pioneering work of Yaghi *et al.* in 2005<sup>1</sup> has initiated studies of covalent organic frameworks (COFs), which have witnessed a resurgence of interest in the last few years due to their application in the energy storage field.<sup>2–6</sup> Among them, two-dimensional (2D-) layered COFs take the lead in the research of solid-state electrolytes (SSEs).<sup>2,6</sup> 2D-COFs are composed of single-layer sheets in which large pores are constructed by organic building blocks interconnected with each other by covalent bonds. The sheets are tightly packed *via* an eclipsed stacking fashion with strong  $\pi$ - $\pi$  interactions, thus yielding a porous yet rigid structure characteristic of periodically aligned tunnels.<sup>7</sup> The high architectural and chemical robustness of 2D-COFs makes them ideal candidates to be employed as the skeleton of SSE in lithium ion batteries (LIBs).<sup>2</sup> The produced SSE can eliminate the threat of dendritic lithium deposition at the anode while providing better interfacial contact with electrodes than inorganic SSEs.<sup>8,9</sup> Although huge leaps have been made in the development of 2D-COF based electrolytes, a fundamental understanding of ion conduction in the Li salts confined in such one-dimensional (1D) tunnels is still lacking.<sup>10,11</sup> Therefore, investigating the mechanism of Li ion traffic in 2D-COF SSE from a theoretical perspective is an important objective in this area and the focus of the current work.

Generally, atoms or ions in a solid phase can hardly move away from their original lattice sites, as they are highly condensed and essentially immobile. Small ions such as Li<sup>+</sup> ions can only diffuse *via* a hopping mechanism in which the ion is envisioned to jump to an adjacent vacancy in the lattice. This is what we observe in typical SSEs,<sup>12</sup> and differs from the ionic diffusion of traditional ionic conductors in a liquid phase. In liquid electrolyte, ionic components contributing to the conductivity (Li<sup>+</sup> ions) tend to form complex with the solvents, in which case all particles can undergo long-range diffusion.<sup>13</sup> In this work, we demonstrate by performing first principles calculations that although the 2D-COF based electrolyte can be viewed as solid due to the limited migration length of the constituent atoms, the Li<sup>+</sup> ion diffusion inside adopts a liquid-like behaviour with a high ionic mobility driven by the rotation and short-range translation of coordinated anions and solvent molecules. We select LiClO<sub>4</sub> as the Li salt and tetrahydrofuran (THF, C<sub>4</sub>H<sub>8</sub>O) as the solvent, both of which are impregnated into the archetypical COF-5, as shown in Fig. 1a and 1b. The dynamics and microstructural evolution during Li<sup>+</sup> ion diffusion in the constructed SSE are investigated to provide a molecular-level insight of the facile Li<sup>+</sup> ion traffic, which could pave the way for the improved design of 2D-COF based electrolytes regarding the optimal combination between the COF skeleton, Li salt and the organic solvent.

## Results and discussion

The COF-5 corresponds to a composition of C<sub>9</sub>H<sub>4</sub>BO<sub>2</sub> in a formula unit and is composed of sheets that are stacked in

School of Advanced Materials, Peking University, Shenzhen Graduate School, Shenzhen 518055, People's Republic of China. E-mail: lisan@pku.edu.cn, panfeng@pkusz.edu.cn

† Electronic supplementary information (ESI) available. See DOI: 10.1039/c9cp02117e

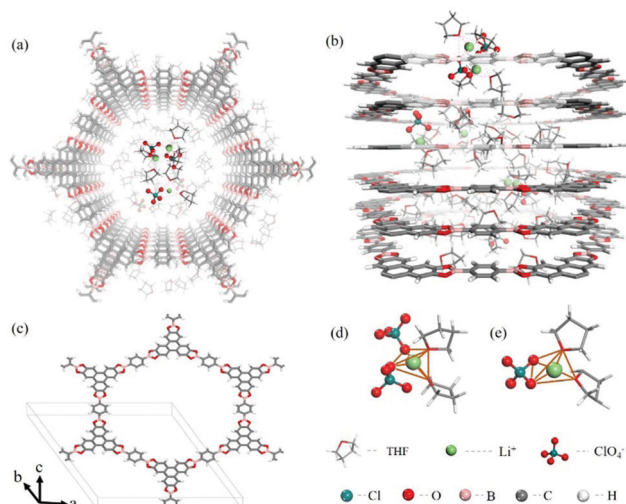


Fig. 1 (a) Top and (b) side views of schematic representation of 1D  $\text{Li}^+$  diffusion in tunnels of 2D-COF filled with Li salt and solvent; (c) the structure of COF-5; (d) and (e) two representative local structures of the coordination environments around a  $\text{Li}^+$  ion.

layer by layer configuration along the  $c$ -axis, forming honeycomb-like structures with pore diameters of nearly 30 Å.<sup>11</sup> In the calculations, a unit cell consisting of 6 formula units is built, as shown in Fig. 1c. In the tunnel perpendicular to the 2D-COF layers,<sup>2</sup>  $\text{LiClO}_4$  and 24 THFs are initially distributed in a random manner, and are equilibrated for 1 ps at 700 K through *ab initio* molecular dynamics (AIMD) simulation before the geometric data are collected over a period of 9 ps at either 300 or 700 K. The AIMD simulation at elevated temperatures with structural parameters fixed to those at 300 K has previously been proved successful in speeding up the diffusion events and capturing the nature of  $\text{Li}^+$  diffusion in electrolytes for LIBs.<sup>12,14</sup> Moreover, the temperature of 700 K is below the critical limit for decomposition of all the chemical entities involved in our work. From the geometric data, two representative structures are selected and shown in Fig. 1d and e after structural optimization. A short-range regularity appears in these configurations where  $\text{Li}^+$  ions are coordinated with four O atoms from either  $\text{ClO}_4^-$  ions or the THFs. The  $\text{O}_4$  tetrahedron bears a strong resemblance to the cases of other Li-salt solutions that have oxygen-containing anions or molecules.<sup>13,15</sup> The Li–O distance are around 2 Å, close to those of conventional liquid and solid electrolytes,<sup>16</sup> indicating a relatively strong electrostatic interaction between  $\text{Li}^+$  ions and the O atoms in both  $\text{ClO}_4^-$  ions and THFs molecules. The pair correlation function between  $\text{Li}^+$  ions and other atoms (see Fig. S1 in the ESI†) illustrates that the first coordination sphere is contributed mostly by Li–O bonds, which encourages us to ignore the influence from atoms outside the  $\text{O}_4$  tetrahedron. The above results also allow us to assume that if the diffusion of the anions and the THFs are restricted, the  $\text{Li}^+$  ions will be tightly encaged in these tetrahedra and faced with relatively large barriers to diffusion. However, this assumption would not be realistic if we consider the rotational dynamics of the  $\text{ClO}_4^-$  ions and THFs, which will be discussed in the following

paragraphs. On the other hand, it should be noted that two of the O atoms in the  $\text{O}_4$  tetrahedron may come from the same  $\text{ClO}_4^-$  ion (Fig. 1e), in which case the Li–O bonds would be slightly stretched (2.04 Å) as compared with those from O atom in THFs (1.94 Å). This is due to the short O–O distance in a  $\text{ClO}_4^-$  ion with steric effects that repel the neighbouring  $\text{Li}^+$  ion. Overall, in the 2D-COF SSE considered in this work, Li ion stays in a  $\text{O}_4$  tetrahedron whose O atoms come from either  $\text{ClO}_4^-$  or THFs with strong Li–O electrostatic interactions.

In the attempt to understand the  $\text{Li}^+$  diffusion in 2D-COF electrolyte, we first calculated the mean square displacement (MSD, denoted by  $\langle \hat{r}^2 \rangle$ ) of  $\text{Li}^+$  ions as a function of time ( $t$ ) from our AIMD simulation at 300 K. The results shown in Fig. 2a clearly illustrate the linear  $t$  dependence of MSD; that is,  $\text{Li}^+$  ions will not simply oscillate inside the  $\text{O}_4$  cages but instead exhibit diffusive behaviour at room temperature, with a diffusion coefficient ( $D$ ) of the order of  $10^{-5} \text{ cm}^2 \text{ s}^{-1}$  according to  $\langle \hat{r}^2 \rangle = 6Dt$ .<sup>17</sup> Such a value is close to those of typical liquid systems<sup>18</sup> and competitive with inorganic SSEs.<sup>19</sup> The linear dependence also indicates that the simulation time in this study is sufficient for the convergence of results on diffusion events. The diffusive behaviour can be further confirmed by the probability density of  $\text{Li}^+$  ions at 700 K, as depicted in Fig. 2b. The probability density defines the time-averaged probability of the spatial distribution of the ions, which is inversely related to the corresponding site energy.<sup>19</sup> We can see that  $\text{Li}^+$  diffusion is mainly confined in the middle region of the tunnels, implying that  $\text{Li}^+$  ions are reluctant to approach the COF-5 framework. A relatively flat energy landscape in the tunnel, as deduced from the continuously

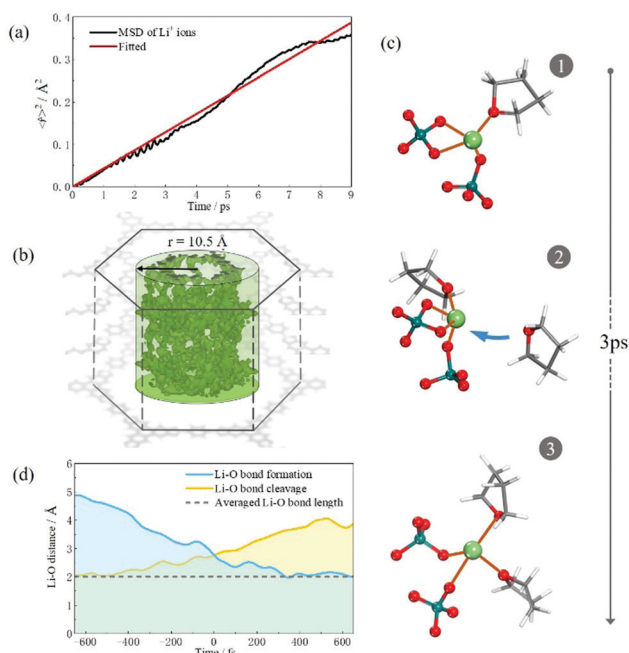


Fig. 2 (a) MSD as a function of time for  $\text{Li}^+$  ions at 300 K, and the corresponding fitted line; (b) the probability density of  $\text{Li}^+$  ions at 700 K; (c) visualization of a representative  $\text{Li}^+$  diffusion event in the AIMD simulation; (d) the distances of the outgoing (Li–O bond cleavage) and incoming (Li–O bond formation) O atoms to the  $\text{Li}^+$  ion, averaged over all diffusion events.

distributed probability density, suggests a low energy barrier for  $\text{Li}^+$  diffusion and therefore a rather facile motion of the  $\text{Li}^+$  ions, which is in consistency with the large diffusion coefficient calculated above. We have calculated the MSD projected onto the  $c$ -axis (Fig. S2, ESI<sup>†</sup>) and the corresponding diffusion coefficient along the tunnels ( $D_{1D}$ ). The 1D ionic conductivity for  $\text{Li}^+$  diffusion along the tunnels can be estimated according to the Nernst–Einstein equation,  $\sigma = cq^2D_{1D}/kT$ , where  $c$  and  $q$  are the concentration and charge of the ions, respectively;  $k$  is the Boltzmann constant and  $T$  is temperature. The conductivity is calculated to be  $0.30 \text{ mS cm}^{-1}$  at 300 K, which agrees well with the experimental value  $(0.26 \text{ mS cm}^{-1})^2$  and demonstrates the fast-ionic conductivity for  $\text{Li}^+$  in 2D-COF SSE.

The fast diffusion of  $\text{Li}^+$  ions might seem contradictory to their jammed state in the  $\text{O}_4$  tetrahedra if the 2D-COF electrolyte is perceived as entirely solid,<sup>12</sup> but a detailed examination of the structures in the vicinity of the  $\text{Li}^+$  ions demonstrates that the microstructural evolution is more liquid-like than expected. A mechanistic picture of  $\text{Li}^+$  diffusion is shown in Fig. 2c, which presents the snapshots of configurations spanning a sequence of about 3 ps. It is noted that the diffusion of  $\text{Li}^+$  is accompanied by the concomitant cleavage and formation of the Li–O coordination bonds, and can be conceptualized as a sequence of well-defined steps. Firstly, the neighbouring  $\text{ClO}_4^-$  ions and THFs are rotated slightly, leaving a relatively large bottleneck for  $\text{Li}^+$  to diffuse. Then the  $\text{Li}^+$  ion is squeezed out of the tetrahedron with the loss of one O linker and simultaneously binds to another linker nearby. The new local configuration is further relaxed to thermodynamic equilibrium, during which the  $\text{Li}^+$  ion spontaneously moves to its final position. This diffusion mechanism is reminiscent of liquid organic salts,<sup>20</sup> and evidently differs from the hopping model of typical SSEs.<sup>12</sup> It appears that although the COF-5 framework presents itself as a solid phase, the  $\text{Li}^+$  ions inside can diffuse as freely as they are in liquid solvents.

In order to quantitatively characterize the transient dynamics of the  $\text{Li}^+$  diffusion events, we plotted the average distances of the outgoing and incoming O atoms to the  $\text{Li}^+$  ion ( $d_{\text{outgoing}}$  and  $d_{\text{incoming}}$ ) from all the  $\text{Li}^+$  diffusion events in our simulation, as shown in Fig. 2d. We defined the reference time  $t = 0$  when the  $\text{Li}^+$  ion is equidistant from both the outgoing and incoming O atoms; in other words, for  $t < 0$  the  $\text{Li}^+$  ion is closer to the outgoing O while for  $t > 0$  to the incoming one. The plot shows that the diffusion event lasts for approximately 1 ps, and that the Li–O distance at  $t = 0$  is smaller than  $(d_{\text{outgoing}} + d_{\text{incoming}})/2$  at  $|t| \approx 0.5 \text{ ps}$  (about  $3 \text{ \AA}$ ). The relatively short Li–O distance at  $t = 0$  means that the  $\text{Li}^+$  ion could be regarded as bonded to both O atoms by electrostatic forces. Therefore, the breaking of old Li–O bond in the old  $\text{O}_4$  tetrahedron and the reforming of new bond in the new tetrahedron occur in parallel, from which follows that the  $\text{Li}^+$  diffusion and the translational/rotational motion of neighbouring  $\text{ClO}_4^-$  ions and THFs should be regarded as concerted, rather than successive. The above scenario is similar to the molecular diffusion mechanism of water reorientation in liquid phase,<sup>21</sup> and substantiates our claim that the  $\text{Li}^+$  diffusion is indeed liquid-like.

Further investigation of the dynamics of  $\text{Li}^+$  diffusion warrants elucidating the mechanism by which the  $\text{ClO}_4^-$  ions and THFs

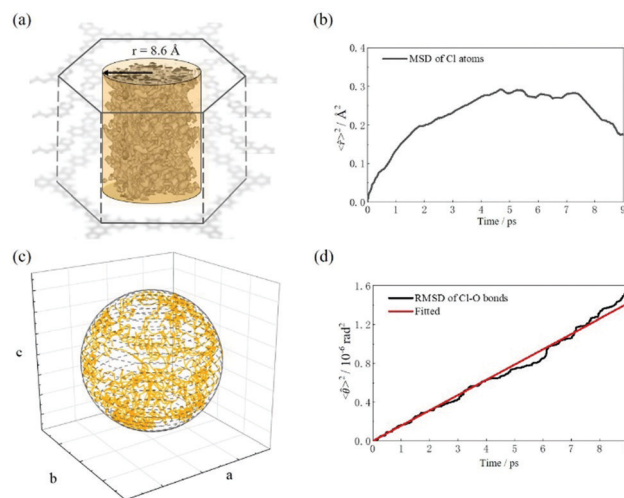


Fig. 3 (a) The probability density of Cl atoms at 700 K; (b) MSD as a function of time for Cl atoms at 300 K; (c) angular trajectory of Cl–O bonds mapped onto the surface of a unit sphere; (d) RMSD as a function of time for Cl–O bonds.

regulate the diffusion events. Fig. 3a presents the probability density of Cl atoms in the  $\text{ClO}_4^-$  ions at 700 K. It is clearly seen that the Cl atoms can only access a small region in the middle of the tunnels, with the radius of the enclosed region slightly larger than one half of the tunnel radius. The spatial region falls well inside that of  $\text{Li}^+$  ions as shown in Fig. 2b, with a radius difference of about  $2 \text{ \AA}$ . It means that  $\text{Li}^+$  cannot access regions at distance  $> 2 \text{ \AA}$  from the  $\text{ClO}_4^-$  ions, indicating that there is a strong correlation between  $\text{Li}^+$  diffusion and the distribution of  $\text{ClO}_4^-$  ions. This can be rationalized by the electrostatic attraction between the two oppositely charged species, which requires that each  $\text{Li}^+$  ion must be accommodated in the vicinity of  $\text{ClO}_4^-$  ions. The translational motion of  $\text{ClO}_4^-$  ions at room temperature is revealed by the MSD of the Cl atoms shown in Fig. 3b. The MSD reaches its maximum value of less than  $0.3 \text{ \AA}^2$  and then starts to decrease, which reflects the non-linearity of the MSD plot and implies the absence of long-range diffusive dynamics of the Cl atoms. Nevertheless, short-range motion is still possible due to the weak interaction between  $\text{ClO}_4^-$  ions and their neighbouring particles. This scenario, similar to those found in amorphous solid systems,<sup>20,22</sup> bolsters our notion that the constructed electrolyte is a substantially solid material with the anions unable to diffuse freely in the tunnels.

In order to describe the rotational movement of  $\text{ClO}_4^-$  ions, we display in Fig. 3c the angular trajectory of all Cl–O bonds projected onto the surface of a unit sphere. It is found that the angular trajectory performs a random walk despite the anisotropic structure of COF-5. In line with Mazza *et al.*,<sup>23</sup> we define the rotational displacement vector  $\langle \hat{\theta} \rangle^2$  of a Cl–O bond at time  $t$  as the sum of rotation vectors of the Cl–O bond for all time steps before. The rotational mean square displacement (RMSD,  $\langle \hat{\theta} \rangle^2$ ) at room temperature is plotted as a function of  $t$  in Fig. 3d, which indicates a linear relationship corresponding to the Einstein equation.<sup>17</sup> Therefore, it can be inferred that the rotational motion of  $\text{ClO}_4^-$  ions is purely diffusive in character,



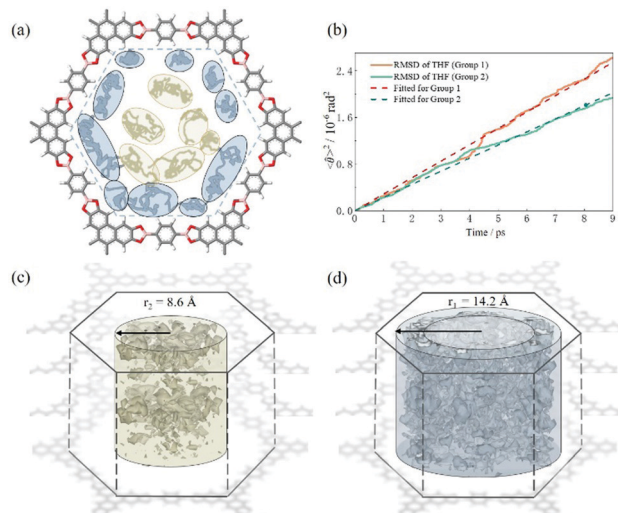


Fig. 4 (a) The trajectory of the centers of THFs projected onto the *ab* plane; (b) RMSD as a function of time for C–O bonds in THFs at 300 K; probability densities of the centers of THFs (c) inside an overlapping region with that of  $\text{ClO}_4^-$  ions (Group 1), or (d) close to the walls of COF-5 (Group 2).

in contrast to their translational motion. The rotational correlation time is estimated to be relatively short (3.4 ps, close to that of liquid water<sup>24</sup>) using the calculated orientational autocorrelation function shown in Fig. S3 (ESI<sup>†</sup>). Such a regime of free rotation of the  $\text{ClO}_4^-$  ions, acting as if they are small balls in the tunnel, can potentially be the facilitator for the fast diffusion of the  $\text{Li}^+$  ions and may unveil the underlying physics of fast  $\text{Li}^+$  transport in 2D-COF SSEs.

Next, we investigate the dynamic features of the THFs through the inspection of their spatial distribution at 700 K. The trajectory of the centres of THFs projected onto the *ab* plane is shown in Fig. 4a, which clearly demonstrates a non-percolating network exhibiting relatively small intersections between the domains of different THFs (elliptical regions). This suggests low translational mobility of the THFs in the tunnels, especially those near the walls of COF-5. Accordingly, we categorize the THFs into two groups: those in the middle region with a radius of 8.6 Å (Group 1) and those outside (Group 2). Analogous to  $\text{ClO}_4^-$  ions, the THFs in both groups permit free rotation during  $\text{Li}^+$  ion diffusion, as reflected by the RMSD of C–O bonds shown in Fig. 4b.

The THFs should be regarded as another kind of balls in the electrolyte, yet they can contribute beyond that. THFs in Group 1 (Fig. 4c) participate in building the  $\text{O}_4$  tetrahedra inside an overlapping region with that of  $\text{ClO}_4^-$  ions, playing there the same role as the latter in regulating  $\text{Li}^+$  ion diffusion. Similar claims can be applied to THFs in Group 2 (Fig. 4d), except that they lie in a region where no  $\text{ClO}_4^-$  ion can access. However, a more important role may be the isolation effect of THFs in Group 2 for partitioning between the ions and COF-5. For the sake of comparison, we have considered the cases where no THF is impregnated into COF-5 and either  $\text{Li}^+$  or  $\text{ClO}_4^-$  is fixed at different positions inside the tunnel (Fig. S4 and S5, ESI<sup>†</sup>). It is found that while  $\text{Li}^+$  shows energetic preference for sites near the COF-5 framework,  $\text{ClO}_4^-$  tends to stay far away from the walls and arrange itself in the interior region. We may assume

that the  $\text{O}_4$  tetrahedra constructed by  $\text{ClO}_4^-$  ions and THFs can screen the interaction between  $\text{Li}^+$  and COF-5, thus eliminating the energy difference for  $\text{Li}^+$  at different sites inside the 2D-COF SSE. In this context, THFs in Group 2 can be regarded primarily as a result of the repulsion between  $\text{ClO}_4^-$  ions and COF-5. Moreover, they can also function as lubricants to improve the wettability of Li salts with COF-5 and circumvent the retarding effects of the solid walls on  $\text{Li}^+$  diffusion and  $\text{ClO}_4^-$  rotation. The retarding effects on THFs in Group 2 can be manifested by their slightly lower rotational mobility as compared with Group 1 (Fig. 4b). The slowdown of molecules in the vicinity of the framework has also been reported for methanol confined in carbon nanotubes.<sup>18</sup>

It is worth mentioning that the scenario where  $\text{Li}^+$  and  $\text{ClO}_4^-$  ions are confined in the interior region of the tunnel is supported by previous experimental measurements using solid-state nuclear magnetic resonance (ssNMR) spectrum.<sup>2</sup> The ssNMR spectrum has suggested a single environment for  $\text{Li}^+$ , which corresponds to the  $\text{O}_4$  tetrahedron as revealed in this work. Going beyond the experimental evidence, our atomistic simulation has indicated that the rotational motion of THFs in Group 2 is indispensable for establishing the confined region and maintaining the facile diffusion of  $\text{Li}^+$  ions when they are close to the walls of COF-5. We believe that the mechanism of partitioning between the ions and the framework is valid in principal in other COF based SSEs, no matter what kinds of medium is used, from small molecules like THFs to polymer chains like polyethylene glycol that has recently been reported.<sup>25</sup>

As mentioned above, the  $\text{Li}^+$  diffusion is liquid-like although the 2D-COF based electrolyte as whole is solid-like. In fact, the  $\text{Li}^+$  ion traffic in 2D-COF SSE seems to combine features of both liquid organic and solid inorganic electrolytes (Fig. 5). On one hand, the local environment of  $\text{Li}^+$  ions (Fig. 5b) resembles those in liquid phase (Fig. 5a) and corresponds to a flatter energy landscape than the inorganic crystalline electrolytes like  $\text{Li}_7\text{La}_3\text{Zr}_2\text{O}_{12}$  (Fig. 5c). On the other hand, the rigid COF skeleton suppresses the long-range diffusion of the solvents and anionic species, thus prohibiting the formation of aggregates that impact ionic conductivity. Some researchers have conjectured that owing to electrostatic interactions,  $\text{Li}^+$  in the COF tunnels would carry along with them the anions during their diffusion,<sup>6</sup> but this may not be true. Our results demonstrate that as long as the Li salts are well dispersed in the solvents, the anions will not behave in a

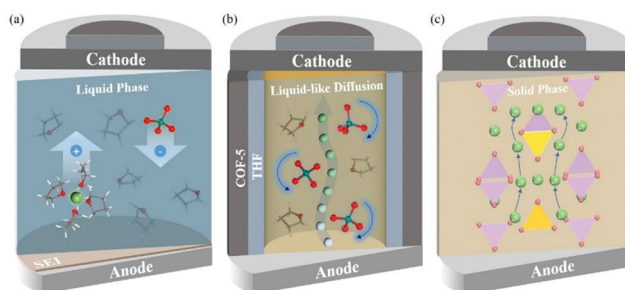


Fig. 5 Schematic graphs of (a) a typical liquid organic electrolyte, (b) 2D-COF SSE where  $\text{Li}^+$  diffusion is liquid-like, and (c) a solid inorganic electrolyte for LIBs.

liquid-like manner except for the rotational motion. This allows us to categorize the 2D-COF electrolyte into the group of SSE, as other researchers did.<sup>2</sup> The hindered translational motion of small molecules confined in 1D tunnels, such as carbon nanotubes, has also been demonstrated in previous studies,<sup>18</sup> which indicates the essential role of nano-size effect on regulating the dynamics of small molecules. In addition, one may tailor the ionic conductivity by changing the Li salts and the radius of the tunnels of COF materials. The limited spatial region of the anions will inevitably pose a problem to reach high ionic conductivity, since the increased concentration of Li salts would compromise the amount of solvents and lead to sluggish motion of the ions. The obvious solutions are to reduce the particle size of the anionic species and to increase the pore size of the COF skeleton. Nevertheless, since the restricted translational motion of the anions and solvents can be attributed to the nano-size effect imposed by COF, the above means may promote translational mobility to the particles and cause aggregations during battery operation. The proper selection of both size parameters, as well as the amount of solvents, could be the keys to developing high-performance 2D-COF SSEs and as such necessitates future efforts of exploration.

## Conclusions

In summary, we have employed AIMD simulation to discern the dynamics and microstructural evolution during Li<sup>+</sup> ion diffusion in a 2D-COF based electrolyte constructed by COF-5, LiClO<sub>4</sub> and THFs. Although the ClO<sub>4</sub><sup>-</sup> ions and THFs in the electrolyte do not exhibit diffusive motion over long distances, the Li<sup>+</sup> ion diffusion adopts a liquid-like behaviour with a diffusion coefficient of the order of 10<sup>-5</sup> cm<sup>2</sup> s<sup>-1</sup>. This behaviour stems from the free rotational and short-range translational motion of ClO<sub>4</sub><sup>-</sup> ions and THFs, and the isolation effect of THFs for partitioning between the ions and COF. The localized spatial distribution of LiClO<sub>4</sub> can be the limiting factor in enhancing the ionic conductivity, which illustrates the importance of tunnel size of COF and the matching solvents in the design of COF based electrolyte systems and thus warrants future studies.

## Conflicts of interest

There are no conflicts to declare.

## Acknowledgements

National Key R&D Program of China (2016YFB0700600), Shenzhen Science and Technology Research Grant (ZDSYS201707281026184), and Guangdong Key-lab Project (No. 2017B0303010130).

## Notes and references

- 1 A. P. Côté and O. M. Yaghi, *et al.*, Porous, Crystalline, Covalent Organic Frameworks, *Science*, 2005, **310**, 1166–1170.
- 2 D. A. Vazquez-Molina and F. J. Uribe-Romo, *et al.*, Mechanically Shaped Two-Dimensional Covalent Organic Frameworks Reveal Crystallographic Alignment and Fast Li-Ion Conductivity, *J. Am. Chem. Soc.*, 2016, **138**, 9767–9770.
- 3 X. Zhan and Q. Zhang, *et al.*, Recent Progress in Two-Dimensional Cofs for Energy-Related Applications, *J. Mater. Chem. A*, 2017, **5**, 14463–14479.
- 4 Q. Xu and D. Jiang, *et al.*, Ion Conduction in Polyelectrolyte Covalent Organic Frameworks, *J. Am. Chem. Soc.*, 2018, **140**, 7429–7432.
- 5 Z. Lei and Y. Wang, *et al.*, Boosting Lithium Storage in Covalent Organic Framework Via Activation of 14-Electron Redox Chemistry, *Nat. Commun.*, 2018, **9**, 576.
- 6 H. Chen, *et al.*, Cationic Covalent Organic Framework Nanosheets for Fast Li-Ion Conduction, *J. Am. Chem. Soc.*, 2018, **140**, 896–899.
- 7 C. S. Diercks and O. M. Yaghi, *et al.*, The Atom, the Molecule, and the Covalent Organic Framework, *Science*, 2017, 355.
- 8 L. Yue and L. Chen, *et al.*, All Solid-State Polymer Electrolytes for High-Performance Lithium Ion Batteries, *Energy Storage Mater.*, 2016, **5**, 139–164.
- 9 X. Liu and X. Li, *et al.*, Recent Progress of Hybrid Solid-State Electrolytes for Lithium Batteries, *Chem. – Eur. J.*, 2018, **24**, 18293–18306.
- 10 J. W. Colson and W. R. Dichtel, Rationally Synthesized Two-Dimensional Polymers, *Nat. Chem.*, 2013, **5**, 453–465.
- 11 P. J. Waller and O. M. Yaghi, *et al.*, Chemistry of Covalent Organic Frameworks, *Acc. Chem. Res.*, 2015, **48**, 3053–3063.
- 12 Z. Deng and S. P. Ong, *et al.*, Computational Studies of Solid-State Alkali Conduction in Rechargeable Alkali-Ion Batteries, *NPG Asia Mater.*, 2016, **8**, e254.
- 13 L. D. Xing and D. Bedrov, *et al.*, Electrode/Electrolyte Interface in Sulfolane-Based Electrolytes for Li Ion Batteries: A Molecular Dynamics Simulation Study, *J. Phys. Chem. C*, 2012, **116**(45), 23871–23881.
- 14 P. Canepa and G. Ceder, *et al.*, Elucidating the Structure of the Magnesium Aluminum Chloride Complex Electrolyte for Magnesium-Ion Batteries, *Energy Environ. Sci.*, 2015, **8**, 3718–3730.
- 15 O. Borodin and K. Xu, *et al.*, Modeling Insight into Battery Electrolyte Electrochemical Stability and Interfacial Structure, *Acc. Chem. Res.*, 2017, **50**(12), DOI: 10.1021/acs.accounts.7b00486.
- 16 V. Chaban, Solvation of lithium ion in dimethoxyethane and propylene carbonate, *Chem. Phys. Lett.*, 2015, **1–5**, 631–632.
- 17 A. Einstein, The Motion of Elements Suspended in Static Liquids as Claimed in the Molecular Kinetic Theory of Heat, *Ann. Phys.*, 1905, **17**, 549–560.
- 18 V. V. Chaban and O. N. Kalugin, Structure and dynamics in methanol and its lithium ion solution confined by carbon nanotubes, *J. Mol. Liq.*, 2009, **145.3**, 145–151.
- 19 Y. Wang and G. Ceder, *et al.*, Design Principles for Solid-State Lithium Superionic Conductors, *Nat. Mater.*, 2015, **14**, 1026–1031.
- 20 R. Gaillac and F.-X. Coudert, *et al.*, Liquid Metal-Organic Frameworks, *Nat. Mater.*, 2017, **16**, 1149–1154.

- 21 D. Laage and J. T. Hynes, A Molecular Jump Mechanism of Water Reorientation, *Science*, 2006, **311**, 832–835.
- 22 F. Faupel and H. Teichler, *et al.*, Diffusion in Metallic Glasses and Supercooled Melts, *Rev. Mod. Phys.*, 2003, **75**, 237–280.
- 23 M. G. Mazza and H. E. Stanley, *et al.*, Relation between Rotational and Translational Dynamic Heterogeneities in Water, *Phys. Rev. Lett.*, 2006, **96**, 057803.
- 24 J. Ropp, *et al.*, Rotational Motion in Liquid Water Is Anisotropic?: A Nuclear Magnetic Resonance and Molecular Dynamics Simulation Study, *J. Am. Chem. Soc.*, 2001, **123.33**, 8047–8052.
- 25 Z. Guo, *et al.*, Fast Ion Transport Pathway Provided by Polyethylene Glycol Confined in Covalent Organic Frameworks, *J. Am. Chem. Soc.*, 2019, **141.5**, 1923.